Chapter 6

Coupling to chiral electrokinetic chromatography:

Quenched phosphorescence detection of methotrexate

M. Castro-Puyana, I. Lammers, J. Buijs, C. Gooijer, and F. Ariese
Analytical and Bioanalytical Chemistry **2011,** *400*, 2913-2919

Abstract

Quenched phosphorescence was used, for the first time, as detection mode in the chiral separation of methotrexate (MTX) enantiomers by electrokinetic chromatography. The detection is based on dynamic quenching of the strong emission of the phosphorophore 4-bromo-1-naphthalenesulfonate (BrNS) by MTX under deoxygenated conditions. The use of a background electrolyte with 3 mg mL^{-1} 2-hydroxypropyl-β-cyclodextrin and 20% methanol in 25 mM phosphate buffer (pH 7.0) allowed the separation of L-MTX from its enantiomeric impurity D-MTX with sufficient resolution. In the presence of 1 mM BrNS, for both enantiomers a detection limit of 3.2×10^{-7} M was achieved, about an order of magnitude better than published based on UV absorption. The potential of the method was demonstrated with a degradation study and an enantiomeric purity assessment of L-MTX. Furthermore, L-MTX was determined in a cell culture extract as a proof-of-principle to show the applicability of the method to biological samples.

6.1 Introduction

L-Methotrexate (L-MTX; Figure 6.1) is an antimetabolite of folic acid that is widely used for the treatment of several cancers, including childhood leukemia, head and neck cancer, and micrometastases of osteosarcoma. More recently, it is also used at low dose for the treatment of rheumatoid arthritis, psoriasis, and steroid-dependent asthma.[1-3] L-MTX acts by inhibiting the enzyme dihydrofolate reductase due to its greater affinity for this enzyme than the closely related folic acid. This leads to a disruption of the folate biosynthesis and key reactions in cell division are shut down in the presence of L-MTX.[4] The D-enantiomer (D-MTX) is subject to significantly different pharmacokinetics; it has a similar inhibitory effect on dihydrofolate reductase, but its antitumor effect is reduced.[1,5] Therefore, D-MTX is considered as a chiral impurity of L-MTX, which can originate from the synthesis of L-MTX or from racemization during the shelf life of the pharmaceutical product under improper storage conditions.[6] Regulatory requirements regarding the purity of chiral drugs have generally become stricter in recent years. Therefore, the development of analytical methodologies to test for enantiomeric impurities in pharmaceutical formulations is of great importance.

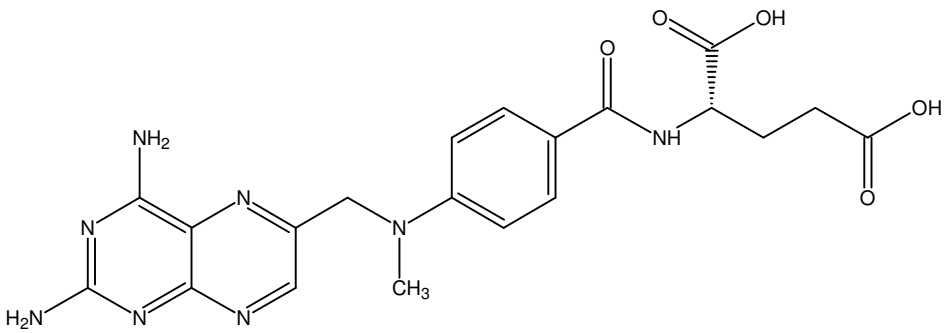

Figure 6.1: Molecular structure of L-methotrexate.

Among the analytical techniques currently used for purity control of chiral pharmaceuticals, electrokinetic chromatography (EKC) is a powerful tool in the field of chiral separations.[7-17] The concentration sensitivity of absorption detection, which is still used most often in capillary electrophoresis (CE), is limited by the optical path length of the capillary and the extinction coefficient of the analytes. For compounds with a chromophoric group, concentration limits in the micromolar range may be achieved in the most favorable cases.[18] Such detection limits may not be sufficiently low for biomedical samples or for the detection of low concentrations of enantiomeric impurities. Therefore, in this chapter we investigate whether luminescence methods without chemical derivatization can provide a suitable alternative.

Room-temperature phosphorescence (RTP) in deoxygenated liquid solutions is an attractive luminescence spectroscopic method for detection in CE.[19-27] Apart from direct phosphorescence, in which the analyte is excited and its own phosphorescence is detected,

several indirect phosphorescence modes can be distinguished based on sensitization or quenching. In one sensitized mode, the analyte is excited and transfers its excitation energy to a more strongly phosphorescent acceptor added to the background electrolyte (BGE) after which the emission of the latter is observed.[27] Alternatively, one can excite a donor reagent with excellent absorption properties that can transfer its electronic energy to the analyte of which the emission is detected.[28] Finally, in the quenched mode, a phosphorescent reagent is excited and its phosphorescence quantum yield is reduced due to dynamic quenching by the analyte. This leads to negative peaks in the electropherogram.[20,21,29,30] Importantly, also non-phosphorescent analytes can be detected in quenched phosphorescence. Note that quenched phosphorescence is different from the indirect absorption mode, which is based on the displacement of an absorbing ion in the BGE by analyte ions.

Examination of the literature reveals that chiral discrimination of MTX has been achieved by means of different analytical techniques such as amperometric biosensors,[31] voltammetric methods[32], potentiometric membrane electrodes[1], TLC[33], HPLC[6,34,35], and CE[5,36-39]. In the case of CE, the chiral separation of MTX and other compounds was carried out to evaluate vancomycin[36], D-(+)-tubocurarine[37], and cyclosophoraoses[39] as chiral selectors. Moreover, Kuo *et al.*[38] developed a method for the enantiomeric analysis of MTX in pharmaceuticals using 2-hydroxypropyl-β-cyclodextrin (HP-β-CD) as chiral selector. This method was only applied to verify the content of L-MTX in tablet and injection formulations, but not for purity control. On the other hand, Gotti *et al.*[5] determined achiral and chiral impurities of L-MTX in pharmaceuticals using a micellar EKC system with β-CD.

In this chapter, we explore the applicability of phosphorescence as a detection mode for the chiral EKC separation of MTX. First, the direct and indirect phosphorescence properties of MTX were investigated in batch experiments. The quenched phosphorescence mode was found to be appropriate for the detection of MTX in combination with its chiral separation. In addition, the influence of different experimental conditions on the enantiomeric separation was studied. Finally, the method developed in this chapter was applied to the enantiomeric purity control of L-MTX in a pharmaceutical formulation, to a short-term stability study, and to the determination of L-MTX in a spiked cell culture extract.

6.2 Experimental section

6.2.1 Chemicals

All reagents employed were of analytical quality. Sodium phosphate monobasic, methanol, and β-CD were purchased from Sigma (St. Louis, MO, USA). Sodium hydroxide was obtained from Fluka (Buchs, Switzerland). (±)-Camphorquinone (CQ) and 2-hydroxy-propyl-β-CD (HP-β-CD) were from Aldrich (Steinheim, Germany). 4-Bromo-1-naphthalene-sulfonate (BrNS) was synthesized in-house.[40] Water used for preparing the solutions was purified using a Milli-Q system from Millipore (Bedford, MA, USA). L-MTX was obtained

from Aldrich (Steinheim, Germany), and D-MTX was kindly provided by dr. R. Gotti (University of Bologna, Italy). The pharmaceutical formulation analyzed (Emthexate PF, 100 mg mL^{-1}; Pharmachemie BV, Haarlem, the Netherlands) and the L-MTX containing cell culture extract were kindly provided by dr. G. Jansen and I. Kathman (VU Medical Center, Amsterdam, the Netherlands).

6.2.2 Batch experiments

A Cary Eclipse luminescence spectrometer (Varian, Melbourne, Australia) equipped with a pulsed xenon lamp was used for the batch experiments. The samples were deoxygenated using a stable nitrogen flow in a long-necked cuvette with a stopper and narrow vent (Hellma, Müllheim, Germany). The temperature was kept at 20°C using the single-cell Peltier cooler of the spectrometer. The phosphorescent reagents BrNS and (±)-CQ were excited at 294 or 470 nm, respectively. Excitation and emission band widths were set to 10 nm and the PMT voltage was 600 V. To avoid detecting interfering scatter and fluorescence, a delay time of 0.1 ms was used. The gate time was set at 5.0 ms. For the lifetime measurements, the initial delay time and the gating time intervals were set at 0.05 ms. Decay curves were fitted in OriginPro 8.0.

6.2.3 Capillary electrophoresis

EKC separations were carried out using a CE system (200 series; Prince Technologies, Emmen, the Netherlands) and an uncoated fused-silica capillary (Polymicro, Phoenix, AZ, USA) with an inner diameter of 75 μm, an outer diameter of 375 μm, and a total/effective length of 110/60 or 120/70 cm. The measurements were performed at room temperature, the voltage applied was 30 kV, and the samples were injected by pressure (50 mbar for 0.08 min). Since deoxygenation is required to observe RTP, a modified vial was used to purge the buffer solution continuously with nitrogen.[19] The nitrogen flow rate was kept constant with a flow regulator. Before first use, a capillary was rinsed with 1 M NaOH for 30 min, followed by 2 min with deionized water, 60 min with the buffer, and 5 min with the BGE (purged with nitrogen for at least 10 min before the start of the analysis and during the separation to remove oxygen). The capillary was rinsed with BGE for 2 min between runs. All solutions were filtered through 0.2-μm syringe filters (Whatman, Dassel, Germany) before their use in the CE system.

An LS40 luminescence LC detector (Perkin-Elmer, Beaconsfield, U.K.), adapted for CE,[30] was used as phosphorescence detection system. The delay time was 0.08 ms and the gating time 3.00 ms. Lamp excitation was performed at 294 nm and emission was collected by means of the total emission mirror and the 390-nm long-pass filter provided with the instrument.

6.2.4 Procedure

Running buffers were prepared by dissolving sodium phosphate in deionized water, adjusting the pH to 7.0 with 1 M NaOH before completing the volume to get a concentration of 25 mM. BGEs were prepared by dissolving the cyclodextrins in the buffer solution. Stock solutions of 0.025 M BrNS and 0.1 M (±)-CQ were prepared in water and methanol, respectively, and stored at 5°C. Stock solutions of L-MTX or D-MTX were prepared by dissolving each enantiomer in 0.1 M NaOH up to a final concentration of 10^{-3} M and stored at -20°C. Aliquots were diluted in water to get solutions with the desired concentrations (using an L/D ratio of 2:1 for easy distinction of the two peaks).

Human CEM leukemia cells (5×10^6 CEM-WT) were centrifuged (528×*g* for 5 min at room temperature), and the pellet was washed with 20 mL (4°C) Hanks balanced salt solution (HBSS) buffer containing 20 mM HEPES, 140 mM NaCl, 6 mM KCl, 2 mM $MgCl_2$, and 6 mM glucose, set with NaOH to pH 7.4. After centrifugation (528×g for 5 min at 4°C), the pellet was resuspended in 1 mL HBSS (4°C) followed by centrifugation (15,294×*g* for 5 min at 4°C). The pellet obtained was resuspended in 150 µL HBSS (4°C) and spiked with 1 µM MTX and 40 µL ice-cold 40% trichloroacetic acid. After 20 min, the cell suspension was shaken and centrifuged at 15,294×*g* for 5 min at 4°C, and the supernatant was separated and suspended in alamine/freon. Finally, the aqueous layer was separated by centrifugation (15,294×*g* for 5 min at 4°C) and stored at -20°C.

6.3 Results and discussion

6.3.1 Batch experiments

According to the literature, the enantiomeric separation of MTX by EKC can be achieved using HP-β-CD as chiral selector in phosphate buffer (pH 7.0).[38] Keeping in mind that the objective of this chapter was to investigate the feasibility of phosphorescence detection in CE as an alternative to absorption detection, we employed these preliminary conditions to study the direct and indirect phosphorescence of MTX in batch.

First of all, the absorption and fluorescence spectra were recorded in order to find the optimum excitation conditions. Four absorption maxima were discerned at 220, 259, 303, and 373 nm (data not shown). The fluorescence of MTX under the experimental conditions was too weak to be of interest from an analytical detection point of view. Interestingly though, instead of a single fluorescence emission band as generally expected, two weak emission bands were found at 356 and 465 nm (data not shown). This is attributed to the two separate chromophoric moieties of MTX, which are connected by an aliphatic –C–N– group. The corresponding fluorescence excitation spectra are distinctly different: The absorbance maxima at 220 and 303 nm are associated with the 365-nm fluorescence emission band; those at 259 and 373 nm with the 456-nm fluorescence emission band. Thus, there are two suitable

excitation wavelengths for MTX, 303 and 373 nm, corresponding presumably to the benzoyl and the pteridine unit, respectively.

Also two phosphorescence emission signals could be expected. However, no direct phosphorescence was observed at either excitation wavelength under deoxygenated liquid conditions. Therefore, indirect phosphorescence detection based on sensitization or quenching was explored. For this purpose, the phosphorophores BrNS and (±)-CQ were tested; both compounds have been used extensively in earlier studies.[19,21-23,26,28,40,41] In the sensitized phosphorescence mode, MTX is excited and potentially transfers its excitation energy to the phosphorophores BrNS or (±)-CQ, of which the phosphorescence emission is detected. Since 303 nm is very close to the absorption maximum of BrNS (294 nm) and would result in a high phosphorescence background of this acceptor, MTX was only excited at 373 nm in the presence of BrNS. However, no sensitized phosphorescence was observed using BrNS as an acceptor (data not shown). The energy transfer from MTX excited at 303 or 373 nm to (±)-CQ resulted in an only small increase in the (±)-CQ phosphorescence signal (data not shown). Therefore, sensitized phosphorescence is not a promising option for MTX detection either. Presumably, the triplet-state energies of both chromophoric moieties of MTX are too low for efficient transfer to BrNS or (±)-CQ.

In the dynamically quenched phosphorescence mode, BrNS or (±)-CQ is excited at 294 or 470 nm, respectively, and its phosphorescence intensity is monitored. Quenching by MTX diminishes the observed phosphorescence intensity from I_0 to I according to the Stern-Volmer equation

$$\frac{I_0}{I} = 1 + k_q \tau_0 [Q] \qquad \textbf{Eq. 6.1}$$

where k_q is the bimolecular quenching rate constant, $[Q]$ the analyte concentration, and τ_0 the triplet lifetime of the phosphorophore in the absence of quenching analyte.[29,30]

Figure 6.2 shows the phosphorescence emission spectra of BrNS and (±)-CQ in the presence of HP-β-CD with or without 10^{-5} M L-MTX. Under the applied conditions in the absence of quencher, the phosphorescence intensity of BrNS was about 50 times higher than that of (±)-CQ. For both phosphorophores, the presence of L-MTX resulted in a decrease of the signal: I_0/I = 15.3 for BrNS and 1.5 for (±)-CQ. Lifetime measurements showed that in both cases the quenching is dynamic of nature. For instance, the phosphorescence lifetime of BrNS decreased from 2.05 to 0.150 ms in the presence of MTX. This 14-fold decrease is very close to the observed change in intensity. The bimolecular quenching rate constant of BrNS by MTX was 7×10^8 M^{-1} s^{-1}, close to the typical rate constant of collisional quenching ($1\text{-}5\times10^9$ M^{-1} s^{-1}). In dynamically quenched phosphorescence detection for CE, a high background signal and a long triplet lifetime τ_0 are preferred for maximum sensitivity. Furthermore, the phosphorescence should be efficiently quenched by the analytes. Therefore,

BrNS was selected as background phosphorophore for further experiments with quenched phosphorescence detection.

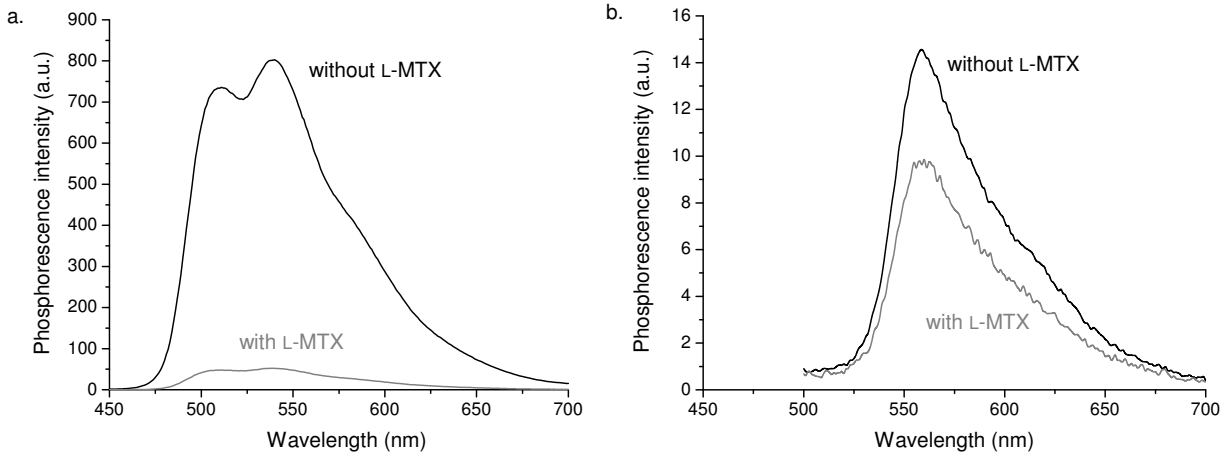

Figure 6.2: Phosphorescence emission spectra of (a) 1×10^{-5} M BrNS and (b) 2 mM (±)-CQ with 1×10^{-5} M L-MTX (gray trace) and without L-MTX (black trace). All samples were made in 25 mM phosphate buffer (pH 7.0) with 3 mg mL^{-1} HP-β-CD and were purged with nitrogen to remove oxygen. A pulsed xenon lamp was used to excite BrNS at 294 nm and (±)-CQ at 470 nm.

6.3.2 Capillary electrophoresis

For the optimization of the CE separation, we started out from the experimental conditions described by Kuo *et al.*[38] with small modifications, such as the use of a longer capillary (at least 60 cm to the detection window instead of 30 cm since short capillary lengths are not practical with the LS40 detector), a higher CE voltage (30 kV), and the presence of 1 mM BrNS in the BGE. At first, only a partial resolution of MTX enantiomers was obtained. Therefore, various parameters such as CD concentration, methanol percentage, and capillary length were studied in order to improve the chiral separation. These aspects were optimized as separate parameters.

The degree of complexation of the enantiomers is affected by the concentration of the chiral selector. Therefore, the influence of the HP-β-CD concentration on the enantioseparation of MTX was investigated in the range from 1 to 10 mg mL^{-1}. The resolution gradually deteriorated when the concentration increased up to 10 mg mL^{-1}. Increasing HP-β-CD concentrations result in shorter migration times because the lower electrophoretic mobility of the <MTX|HP-β-CD> complexes with respect to free MTX leads to a migration closer to the EOF. Eventually, 3 mg mL^{-1} of HP-β-CD was chosen for further experiments as a compromise between resolution and analysis time (data not shown). Interestingly, the peak areas observed with quenched phosphorescence detection were hardly affected by the HP-β-CD concentration, indicating that free and complexed MTX have similar quenching properties toward BrNS. Therefore, no enantioselectivity was observed in the quenched phosphorescence detection of MTX.

To improve the separation further, the addition of different percentages of methanol (10%, 20%, and 25%) was studied. Adding organic modifier to the running buffer may affect the enantiomeric resolution, as well as other parameters such as the EOF, the conductivity of the BGE, and the analysis time. With higher percentages of methanol, the chiral resolution improved, but this added to the analysis time. As a trade-off between both parameters, 20% methanol was chosen for further experiments (data not shown).

However, the enantioseparation of MTX was still only partial. Possibly, the 6-mm detection window of the lamp-based phosphorescence detector contributed to the overall band broadening. Therefore, the detection window was reduced in size by means of black shrink tubing around the capillary. Figure 6.3 shows the electropherograms obtained for a sample containing 5×10^{-6} M L-MTX and 2.5×10^{-6} M D-MTX using different detection window lengths. Reducing the window to about 2 mm improved the resolution, but a significant loss of signal (I_0 and I) was observed with even narrower detection windows. As a compromise, the 2-mm window was chosen for further experiments.

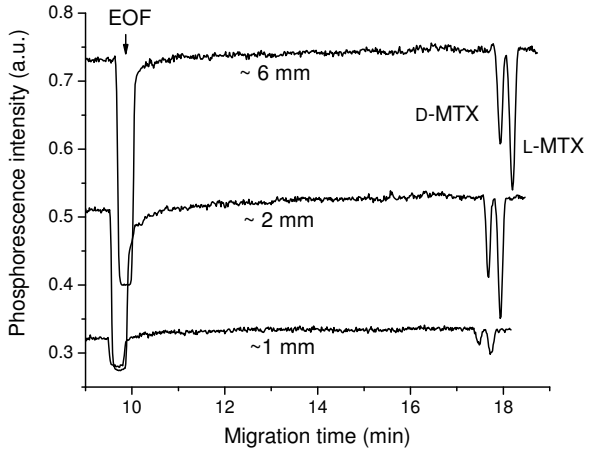

Figure 6.3: Influence of the detection window length (from 1 to 6 mm) on the phosphorescence intensity and the chiral resolution of an EKC separation of a sample containing 5×10^{-6} M L-MTX and 2.5×10^{-6} M D-MTX. A BGE of 1 mM BrNS with 3 mg mL^{-1} HP-β-CD and 20% methanol in 25 mM phosphate buffer (pH 7.0) was used after purging with nitrogen to remove the oxygen. The capillary had a total length of 110 cm and an effective length of 60 cm. Excitation of BrNS at 294 nm was performed with a pulsed xenon lamp. The electropherograms are vertically shifted for clarity.

The capillary length was increased from 60 to 70 cm to further improve the separation. Finally, the variation of the BrNS concentration from 0.5 to 1.5 mM did not show major differences. Since the use of 1.0 mM BrNS resulted in a slightly higher phosphorescence intensity, this concentration was chosen for further experiments (data not shown).

In summary, the chiral separation of the MTX enantiomers monitored with quenched phosphorescence detection was achieved using a BGE of 1 mM BrNS with 3 mg mL^{-1} HP-β-CD and 20% methanol in 25 mM phosphate buffer (pH 7.0) in a capillary of 70 cm to the detector with a detection window of about 2 mm. These conditions allowed the separation

of MTX with a resolution of ~1.5. Finally, the limits of detection and quantification (LOD and LOQ) were calculated from the S/N ratio equal to 3 and 10, respectively, after injecting a sample of 2.5×10^{-6} M L-MTX and 1.25×10^{-6} M D-MTX. LODs of 3.2×10^{-7} M and LOQs of 1.1×10^{-6} M were achieved for both enantiomers. This is a major improvement compared with the LODs reported in the literature for the chiral separation of MTX with absorption detection, including 4×10^{-6} M for CE[38], 1.5×10^{-6} M for MECK[5], and 2×10^{-6} M for HPLC[6].

6.3.3 Application

The developed method was applied to determine the enantiomeric purity of a standard and a pharmaceutical formulation of L-MTX. The level of D-MTX in both samples was quantified by means of the standard addition method. The percentages of spiked D-MTX ranged from 0% to 3% (w/w), relative to a nominal concentration of L-MTX of 10^{-4} M. Figure 6.4 shows the electropherograms of both samples without addition of D-MTX. The actual level of the L-enantiomer was too high to be determined immediately (upper limit of the calibration range is 1×10^{-5} M) and was therefore verified separately after dilution.

The peak heights do not increase linearly with the analyte concentration when using quenched phosphorescence detection. However, linear calibration curves can be obtained by plotting I_0/I versus the percentage of D-MTX ([Q]) added to the sample, according to the Stern-Volmer equation (Equation 6.1). Linear regression analysis gives $I_0/I = 0.228[Q] + 1.25$ ($R^2 = 0.9994$) for the standard and $I_0/I = 0.249[Q] + 1.15$ ($R^2 = 0.9899$) for the pharmaceutical formulation. Percentages of 1.1% (chemical standard) and 0.6% D-MTX (pharmaceutical formulation) were calculated by solving the above equations for $I_0/I = 1$.

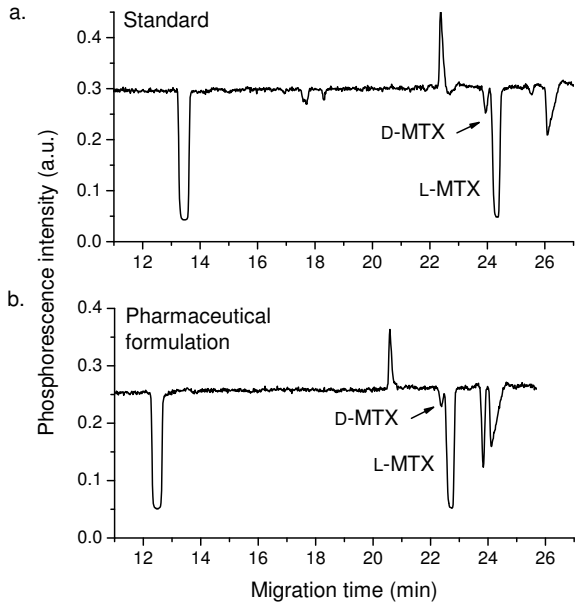

Figure 6.4: Determination of the D-MTX impurity in a (a) L-MTX standard and (b) pharmaceutical formulation. The samples had a nominal L-MTX concentration of 1×10^{-4} M. The capillary had a total length of 120 cm and an effective length of 70 cm. Other experimental conditions as in Figure 6.3.

A short-term degradation study was carried out to investigate the possible racemization of L-MTX. Nine standard samples of 10^{-4} M L-MTX were stored at 4, 20, and 37°C and analyzed after 2, 6, and 24 hours. The D-MTX levels were very similar in all samples (the ratios I_0/I ranged from 1.30 to 1.36), which showed that no significant racemization of L-MTX occurred under the conditions studied.

Finally, as a proof-of-principle experiment for the application of the developed method to biological samples, L-MTX was determined in a cell culture extract from human CEM leukemia cells. The extract was spiked with 1 μM L-MTX, which is a realistic level in pharmacokinetic and pharmacodynamics experiments. As demonstrated in Figure 6.5, the intracellular components caused little interference in the quenched phosphorescence detection of L-MTX. The developed method will be useful for determining the intracellular concentration of MTX and can be applied in future studies on the dynamic equilibrium between influx and efflux routes of this therapeutic drug.

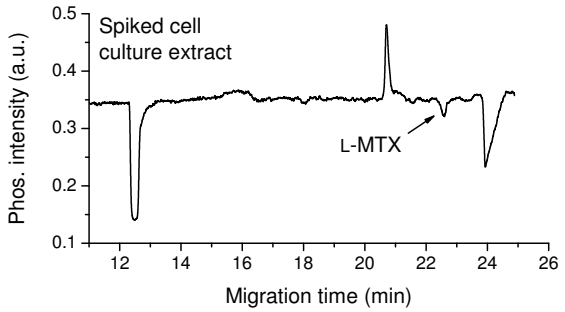

Figure 6.5: Analysis of a cell culture extract spiked with 1 μM L-MTX. Experimental conditions as in Figure 6.4.

6.4 Conclusions

Following the batch study of the phosphorescence characteristics of MTX (direct and indirect phosphorescence), the quenched phosphorescence mode was chosen as the detection method for the chiral separation of the MTX enantiomers by EKC. Under the optimized conditions, 1 mM BrNS with 3 mg mL^{-1} HP-β-CD and 20% methanol in 25 mM phosphate buffer (pH 7.0), the enantiomeric separation of L-MTX and D-MTX was obtained with a resolution of ~1.5. Under these conditions, a LOD of 3.2×10^{-7} M was achieved for both enantiomers, improving the LODs previously reported in the literature with about an order of magnitude. Finally, the developed method was satisfactorily applied to the enantiomeric purity control of a standard and a pharmaceutical formulation of L-MTX. A short-term stability study did not show any major degree of racemization in aqueous solution up to 24 hours, not even at 37°C. The method was also found to be suitable for studying MTX in cell culture extracts.

References

(1) Rat'ko, A. A.; Stefan, R. I.; Van Staden, J. F.; Aboul-Enein, H. Y. *Talanta* **2004**, *64*, 145-150.

(2) Rodríquez Flores, J.; Castañeda Peñalvo, G. ; Espinosa Mansilla, A.; Rodríguez Gómez, M. J. *J. Chromatogr. B* **2005**, *819*, 141-147.

(3) Li, H.; Luo, W.; Zeng, Q.; Lin, Z.; Luo, H.; Zhang, Y. *J. Chromatogr. B* **2007**, *845*, 164-168.

(4) Roach, M. C.; Gozel, P.; Zare, R. N. *J. Chromatogr.* **1988**, *426*, 129-140.

(5) Gotti, R.; El-Hady, D. A.; Andrisano, V.; Bertucci, C.; El-Maali, N. A.; Cavrini, V. *Electrophoresis* **2004**, *25*, 2830-2837.

(6) El-Hady, D. A.; El-Maali, N. A.; Gotti, R.; Bertucci, C.; Mancini, F.; Andrisano, V. *J. Pharm. Biomed. Anal.* **2005**, *37*, 919-925.

(7) Chankvetadze, B. *Capillary electrophoresis in chiral analysis*; Wiley: Chichester, 1997.

(8) Tanaka, Y.; Yanagawa, M.; Terabe, S. *J. High Resol. Chromatogr.* **1996**, *19*, 421-433.

(9) Fanali, S. *J. Chromatogr. A* **2000**, *875*, 89-122.

(10) García-Ruiz, C.; Marina, M. L. In *Analysis and detection in capillary electrophoresis*; Marina. M. L.; Rios, A.; Valcarcel, M. Eds; Elsevier: Amsterdam, 2005; Chapter 13.

(11) Van Eeckhaut, A.; Michote, Y. *Electrophoresis* **2006**, *27*, 2880-2895.

(12) Gübitz, G.; Schmid, M. G. *Electrophoresis* **2007**, *28*, 114-126.

(13) Chankvetadze, B. *J. Chromatogr. A* **2007**, *1168*, 45-70.

(14) Ward, T. J.; Baker, B. A. *Anal. Chem.* **2008**, *80*, 4363-4372.

(15) Gübitz, G.; Schmid, M. G. *J. Chromatogr. A* **2008**, *1024*, 140-156.

(16) Fanali, S. *Electrophoresis* **2009**, *30*, S203-S210.

(17) Chankvetadze, B. *Electrophoresis* **2009**, *30*, S211-S221.

(18) Crego, A. L.; Marina, M. L. In *Analysis and detection in capillary electrophoresis*; Marina. M. L.; Rios, A.; Valcarcel, M. Eds; Elsevier: Amsterdam, 2005; Chapter 5.

(19) Kuijt, J.; Arraez Roman, D.; Ariese, F.; Brinkman, U. A. T.; Gooijer, C. *Anal. Chem.* **2002**, *74*, 5139-5145.

(20) Kuijt, J.; Ariese, F.; Brinkman, U. A. T.; Gooijer, C. *Anal. Chim. Acta* **2003**, *488*, 135-177.

(21) García-Ruiz, C.; Siderius, M.; Ariese, F.; Gooijer, C. *Anal.Chem.* **2004**, *76*, 399-403.

(22) García-Ruiz, C.; Hu, X.; Ariese, F.; Gooijer, C. *Talanta* **2005**, *66*, 634-640.

(23) García Ruiz, C.; Scholtes, M. J.; Ariese, F.; Gooijer, C. *Talanta* **2005**, *66*, 641-645.

(24) Zhang, W. H., Wang, Y.; Jin, W. J. *Talanta* **2007**, *73*, 938-942.

(25) Zhang, W. H.; Wang, Y.; Jin, W. J. *Anal. Chim. Acta* **2008**, *622*, 157-162.

(26) Lammers, I.; Buijs, J.; Van der Zwan, G.; Ariese, F.; Gooijer, C. *Anal. Chem.* **2009**, *81*, 6226-6233.

(27) Castro-Puyana, M.; Lammers, I.; Buijs, J.; Gooijer, C.; Ariese, F. *Electrophoresis* **2010**, *31*, 3928-3936.

(28) Lammers, I.; Buijs, J.; Ariese, F.; Gooijer, C. *Anal. Chem.* **2010**, *82*, 9410-9417.

(29) Kuijt, J.; Ariese, F.; Gooijer, C. In *Analysis and detection in capillary electrophoresis*; Marina, M. L.; Rios, A.; Valcarcel, M. Eds; Elsevier: Amsterdam, 2005; Chapter 7.

(30) Kuijt, J.; Brinkman, U. A. T.; Gooijer, C. *Anal. Chem.* **1999**, *71*, 1384-1390.

(31) Stefan, R. I.; Bokretsion, R. G.; Van Staden, J. F.; Aboul-Enein, H. Y. *Talanta* **2003**, *60*, 983-990.

(32) El-Hady, A. D.; Seliem, M. M; Gotti, R.; El-Maali, N. A. *Sens. Actuators B* **2006**, *113*, 978-988.

(33) Subert, J.; Slais, K. *Pharmazie* **2001**, *56*, 355-360.

(34) Cramer, S. M.; Schornagel, J. H.; Kalghatgi, K. K.; Bertino, J. R.; Horváth, C. *Cancer Res.* **1984**, *44*, 1843-1846.

(35) Brandsteterova, E.; Marcincinova, K.; Lehotay, J.; Zbojova, A.; Halko, J. *Neoplasma* **1993**, *40*, 241-245.

(36) Armstrong, D. W.; Rundlett, K. L.; Chen, J. R. *Chirality* **1994**, *6*, 496-509.

(37) Nair, U. B.; Armstrong, D. W.; Hinze, W. L. *Anal. Chem.* **1998**, *70*, 1059-1065.
(38) Kuo, C. Y.; Wu, H. L.; Wu, S. M. *Anal. Chim. Acta* **2002**, *471*, 211-217.
(39) Lee, S.; Jung, S. *Carbohydr. Res.* **2003**, *338*, 1143-1146.
(40) Kuijt, J.; van Teylingen, R.; Nijbacker, T.; Ariese, F.; Brinkman, U. A. T.; Gooijer, C. *Anal. Chem.* **2001**, *73*, 5026-5029.
(41) Kuijt, J.; Ariese, F.; Brinkman, U. A. T.; Gooijer, C. *Electrophoresis* **2003**, *24*, 1193-1199.